Available online at www.sciencedirect.com
ScienceDirect
JOURNAL OF IRON AND STEEL RESEARCH, INTERNATIONAL. 2015, 22(5): 391-395

Reduction Kinetics of Fine Iron Ore Powder in Mixtures of H_2-N_2 and H_2-H_2O-N_2 of Fluidized Bed

Jian-ming PANG, Pei-min GUO, Pei ZHAO
(Center of Efficient Utilization of Resources by Low-temperature Metallurgy, China Iron and Steel Research Institute Group, Beijing 100081, China)

Abstract: Reduction kinetics of fine iron ore powder in different gas mixtures were investigated in high-temperature fluidized bed at a scale of kilograms. Influence of processing parameters, such as particle size, gas flow velocity, height of charge, temperature, compositions of gas mixture, and percentage of inert components, on reduction kinetics was experimentally determined under the condition of fluidization. The equations for calculating instantaneous and average oxidation rates were deduced. It was found that an increasing H_2O percentage in the gas mixture could obviously decrease the reduction rate because the equilibrium partial pressure of H_2 decreased with increasing content of H_2O in the gas mixture and then the driving force of reduction reaction was reduced. When the H_2 content was high, the apparent reaction rate was so rapid when the average size of iron ore fines was less than 1 mm that the reaction temperature can be as low as 750 ℃; when the average size of iron ore fines was more than 1 mm, a high reaction temperature of 800 ℃ was required. In addition, it was also found that the content of H_2O should be less than 10% for efficient reduction.

Key words: hydrogen; fluidized bed; fine iron ore powder; reduction kinetics

Besides established blast furnace route, direct reduction based on the technology of fluidized bed has become one of the most competitive technology in ironmaking[1,2]. Both poduction efficiency and energy consumption depend on the reduction rate of iron oxide in the gas-based direct reduction process. Thus, the researches on improving reduction rate of iron oxide have received world-wide attention[3-14]. However, less attention has been paid to the gaseous reduction of fine iron ore powder[5,6,10], especially the influence of processing parameters, such as iron ore particle size, gas flow velocity, height of charge, temperature, atmosphere, and content of inert gas, on the reduction kinetics under the condition of fluidization.

In this study, the reduction kinetics of iron ore fines was investigated under a home-made high-temperature fluidized bed at the scale of kilograms in the gas mixtures of H_2-N_2 and H_2-H_2O-N_2, which is expected as a basis for the large scale test.

1 Experimental

Hematite, an Australian iron ore, was used in the study and its composition is shown in Table 1. The particle size of iron ore powder was determined after screening. H_2, H_2O and N_2 with high purity were employed in the test.

The reduction reaction was conducted in a home-made high-temperature fluidized bed, whose schematic diagram is shown in Fig. 1. Temperature, pressure and flow velocity of gas mixture during the reduction varied in this study.

Table 1 Composition and particle size of hematite

TFe/%	SiO_2/%	Al_2O_3/%	CaO/%	MgO/%	P_2O_5/%	S/%	FeO/%	Burning loss/%	Particle size/mm
62.81	3.01	2.18	0.01	0.07	0.202	0.026	0.39	4.85	0—8

Foundation Item: Item Sponsored by National Environmental Protection Public Welfare Profession Scientific Special Plan of China (201209023)
Biography: Jian-ming PANG, Doctor, Senior Engineer; **E-mail**: pangjianming1980@163.com; **Received Date**: October 24, 2013

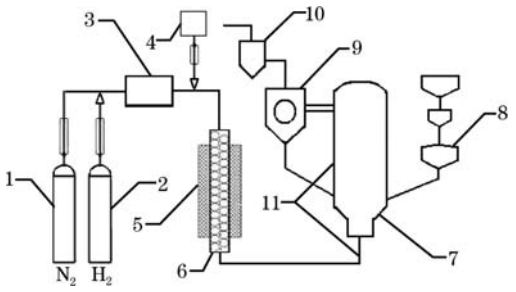

1—N_2 cylinder; 2—H_2 cylinder; 3—Mixing vessel; 4—Steam boiler; 5—Gas pre-heater; 6—Alumina balls; 7—Fluidized bed; 8—Feeder system; 9—Cyclone scrubber; 10—Bag-type dust collector; 11—Temperature sensing location.

Fig. 1 Schematic diagram of the home-made fluidized bed system

The procedure of the test is as follows. A certain amount of fine powder of iron ore is charged to the fluidized bed with feeder facility. Then, the fluidized bed and gas pre-heater are heated to a target temperature. After isothermal holding for several hours at the designed temperature, pure N_2 flows through the fluidized bed for 20—40 min so that the system is free from O_2. After that, switch the pure N_2 flow to the flow of the reducing gas mixture and then maintain for 10—30 min. Finally, switch back to the pure N_2 flow until the system was cooled down to room temperature.

The phases of the product after the reduction reaction were identified by X-ray diffraction (XRD, X'Pert Pro, PANalytical, Co target, $\lambda=0.178897$ nm, 2θ in the range of 20°—80°, and scanning rate of 5 (°)/min). Prior to XRD analysis, the reduced iron fines were ground and then mixed uniformly. Its metallization ratio and reduction degree was calculated by Eqs. (1) and (2), respectively, as suggested in Ref. [14].

$$M=(0.56I_{Fe}+1.56I_{Fe_3C})/(5.14I_{Fe_2O_3}+2.61I_{Fe_3O_4}+0.947I_{Fe_xO}+0.56I_{Fe}+1.56I_{Fe_3C})\times 100\% \quad (1)$$

$$R=(7.71I_{Fe_2O_3}+3.48I_{Fe_3O_4}+I_{Fe_xO})/(7.71I_{Fe_2O_3}+3.915I_{Fe_3O_4}+1.4205I_{Fe_xO}+0.84I_{Fe}+2.34I_{Fe_3C})\times 100\% \quad (2)$$

where, M is the metallization ratio of iron ore fines; R is the reduction degree of iron ore fines; and I is the XRD intensity of corresponding single phase.

The utilization ratio of reducing gas, η, was calculated by Eq. (3) according to the quantity of the ventilated reducing gas, Q_T, and the reduction quantity, Q_R[15].

$$\eta=Q_R/Q_T\times 100\% \quad (3)$$

2 Results and Discussion

2.1 Influence of particle size on reduction kinetics

Fig. 2 describes the influence of particle size on reduction degree and gas utilization ratio after reduction for 10 min at 700 ℃ with the gas velocity (U_g) of 0.8 m·s^{-1}. The reduction degree and gas utilization ratio decrease from 69% and 13.4% to 33.3% and 6.49% respectively when the average size increases from 0.30 to 4.24 mm. Under the same condition, the smaller the average size of iron ore powder, the faster the reaction speed and the higher the utilization ratio of gas. The dependence of reduction degree on the average particle size is similar to that of gas utilization ratio. This is because a smaller average size leads to a larger specific area of iron ore particles, thereby resulting in the decrease of the apparent activation energy of chemical reaction and the increase of the reduction rate and finally the increase of both reduction degree and gas utilization ratio.

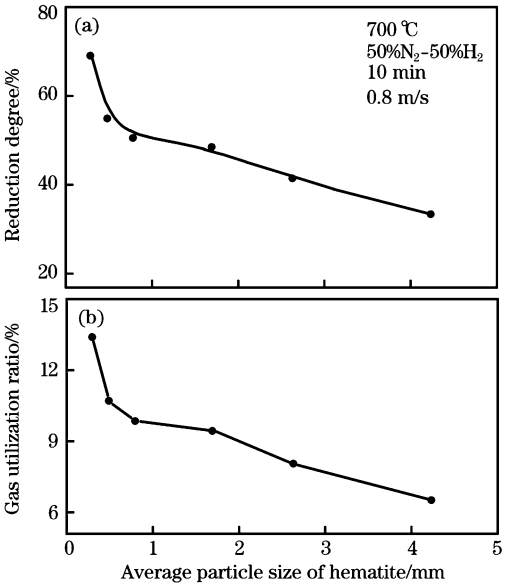

Fig. 2 Influence of particle size on reduction degree and gas utilization ratio

2.2 Influence of hydrogen content on reduction kinetics

In the case of iron ore fines with the average size of 4.24 mm reduced at 750 ℃ for 10 min, the influence of hydrogen content of the gas mixture on reduction degree and gas utilization ratio is given in Fig. 3. The reduction degree increases almost linearly with hydrogen content. For example, the reduction degree at 750 ℃ increases from 34.67% to 70.87% when hydrogen content increases from 40% to 100%, indicating that hydrogen content of the gas mixture has a remarkable influence on the reduction reaction.

The gas utilization ratio decreases with increasing hydrogen content, as shown in Fig. 3(b). When the

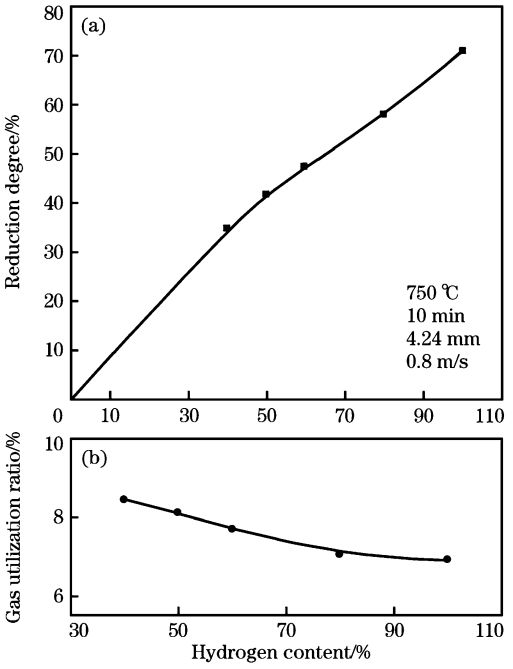

Fig. 3 Influence of hydrogen content on reduction and gas utilization ratio

gas flow velocity is 0.8 m • s^{-1} and the reduction reaction lasts for 10 min, the gas utilization ratio is 8.45% at the hydrogen content of 40% and just 6.91% at the hydrogen content of 100%. This is because higher H_2 content leads to smaller percentage of H_2 consumed for reduction although the reduction degree increases, and therefore, the gas utilization ratio is smaller according to the definition of gas utilization ratio.

2.3 Influence of hydrogen content on reaction rate constant

The reduction reaction of iron oxide by hydrogen is a first-order reaction[15], and the reaction rate is given by

$$\frac{dR}{d\tau}=-\frac{d\varepsilon}{d\tau}=k\varepsilon \tag{4}$$

Integrating the two sides of Eq. (4) leads to

$$\ln\varepsilon-\ln\varepsilon_0=-k\tau \tag{5}$$

Thus,

$$k=\frac{\ln\varepsilon_0-\ln\varepsilon}{\tau} \tag{6}$$

where, ε_0 is the initial proportion of unreacted iron oxide, %; ε is the proportion of unreacted iron oxide, %; τ is the reduction time, s; and k is the constant of apparent reaction rate.

The influence of hydrogen content on k can be calculated by Eq. (6) when the average particle size is 4.24 mm (Fig. 4). It can be seen that the higher hydrogen content of gas mixtures leads to larger k. The relationship between them can be derived as follows by the least-square method.

$$k=(2.194\phi-0.213)/1000\ s^{-1} \tag{7}$$

where ϕ is the hydrogen content in hydrogen-nitrogen mixture, %.

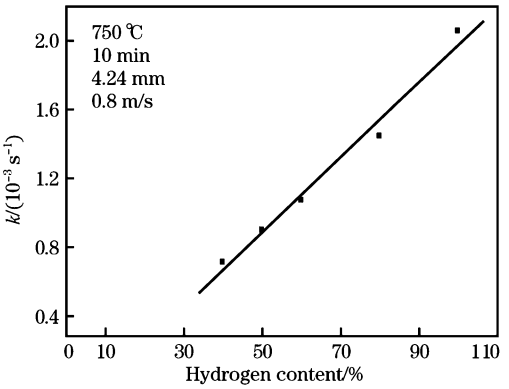

Fig. 4 Influence of hydrogen content on reaction rate constant

2.4 Influence of hydrogen potential on reduction reaction

When iron ore fines with the average size of 1.73 mm are reduced in the gas flow with the gas velocity of 0.8 m • s^{-1} at 700 ℃ for 10 min, the influence of hydrogen potential on gas utilization ratio is shown in Fig. 5. It can be seen that the metallization ratio, reduction degree and gas utilization ratio

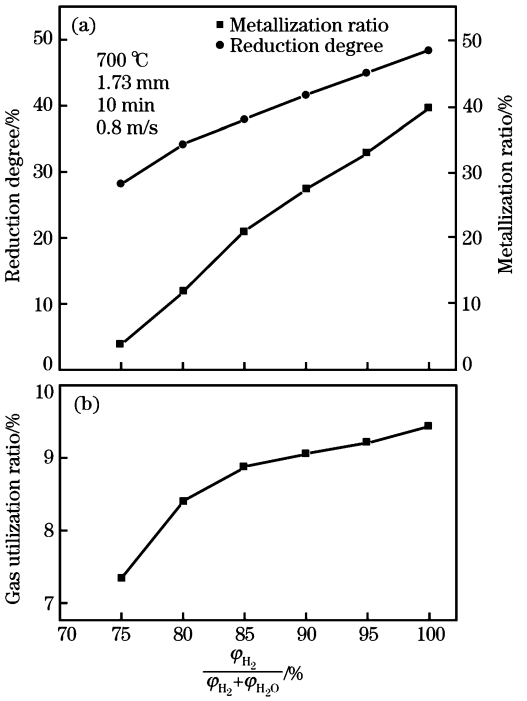

Fig. 5 Influence of reduction potential on iron ore fines reduction and gas utilization ratio

all increase with increasing hydrogen potential because increasing reduction potential, i. e. increasing hydrogen content in the gas mixture, leads to a decrease in water content, and thus, the reduction speed increases due to enhanced reducing capability of gas mixture.

It is also found that the metallization ratio, the reduction degree and the gas utilization ratio are all the largest when the hydrogen potential increases from 75% to 80%.

The previous research showed that the reduction should be an interface-controlled chemical reaction[14]. The relationship between the metallization ratio and hydrogen potential can be given as follows according to the shrinking core model[16]:

$$M=1-\left[1-\frac{\tau}{\rho_0 r_0}\cdot\frac{k_+(1+K)}{K}(44.643\xi x-c_E)\right]^3 \tag{8}$$

where, ρ_0 is the molar concentration of oxygen in the iron ore fines, mol/m^3; r_0 the radius of the particle, m; k_+ is the intrinsic reaction rate constant, m/s; K is the reduction reaction equilibrium constant; ξ is the working hydrogen fraction of the gas mixtures; x is the hydrogen potential fraction, $x=\frac{\varphi_{H_2}}{\varphi_{H_2O}+\varphi_{H_2}}$; and c_E is the equilibrium concentration of reducing gas, mol/m^3.

The measurements and the calculated results on metallization ratio using Eq. (8) are shown in Fig. 6 for various hydrogen potentials. It can be seen that metallization ratio increases with increasing hydrogen potential but the slope tends to decrease slightly. For example, when the water vapour content increases from 0 to 5% in the gas mixtures, the metallization ratio decreases from 39.7% to 27.3%, and the reduction extent is about 31.5%; whilst the water vapour content increases from 5% to 10%, the metallization ratio decreases from 27.3% to 11.8% and the reduction extent is about 56.8%. This can be explained by equilibrium diagram of iron oxide reduction by H_2 and the shrinking-core kinetic model, as discussed below.

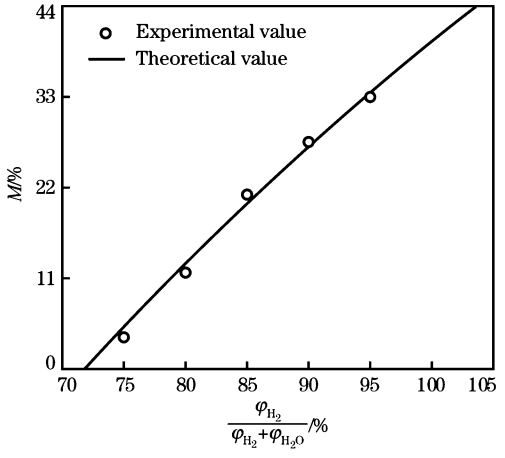

Fig. 6 Comparison between experimental value and theoretical value of influence of hydrogen potential on iron ore fines reduction

Eq. (8) indicates that the metallization ratio of iron ore fines depends on both the reaction rate constant and the reduction potential. The parameters in Eq. (8) do not change during reduction except x and M in the case of constant particle size and temperature. It can be seen from Fig. 7 that the hydrogen potential diminishes with decreasing hydrogen content. The decrease in metallization ratio of iron ore fines due to the varying content of water vapour should be calculated by $N=\frac{(\varphi_{H_2})_1-(\varphi_{H_2})_2}{(\varphi_{H_2})-(\varphi_{H_2})_E}=\frac{\Delta\varphi_{H_2O}}{(\varphi_{H_2})_1-(\varphi_{H_2})_E}$ instead of $N=\frac{(\varphi_{H_2})_1-(\varphi_{H_2})_2}{(\varphi_{H_2})_1}=\frac{\Delta\varphi_{H_2O}}{(\varphi_{H_2})_1}$. Therefore, the influence of hydrogen potential on iron ore fines reduction is more than the contribution resulting from increasing water vapour in the gas mixtures.

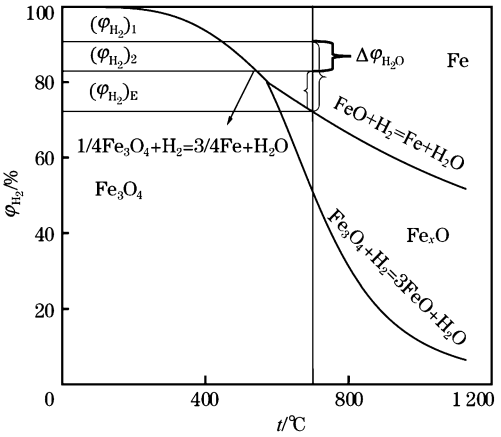

Fig. 7 Equilibrium diagram of iron oxide reduction by H_2

3 Conclusions

(1) The reducing kinetics of the iron ore fines in the fluidization condition was studied. The quantitative relationship between reduction kinetics of ore fines and processing parameters was determined and the formulas for calculating the instantaneous and average oxidation rates were presented.

(2) H_2O in the reducing gas can obviously reduce the apparent reduction rate of ore fines due to the reduced driving force for the reaction at the increasing H_2O content.

(3) When the reducing gas is rich in hydrogen and the average size of iron ore powder is less than 1 mm, the apparent reaction rate constant is so large that the temperature of reaction can be less than 750 ℃; whilst a high temperature of about 800 ℃ is required for reduction reaction when the average size of iron ore powder is more than 1 mm.

(4) The content of H_2O in the gas mixture should be no more than 10% for an efficient reduction reaction.

References:

[1] D. W. Zhang, Fundamental Research on the New Ironmaking Process Based on Fast Reduction at Low Temperature, Central Iron and Steel Research Institute, Beijing, 2007.
[2] X. D. Jin, Iron and Steel 33 (1998) No. 4, 9-12.
[3] R. J. Fruehan, Y. Li, L. Brabie, E. J. Kim, Scand. J. Metall. 34 (2005) 205-212.
[4] A. A. El-geassy, M. I. Nasr, ISIJ Int. 30 (1990) 417-425.
[5] S. K. Dutta, A. Ghosh, ISIJ Int. 33 (1993) 1168-1173.
[6] P. Pourghahramani, E. Forssberg, Thermochim. Acta 454 (2007) 69-77.
[7] A. Pineau, N. Kanari, I. Gaballah, Thermochim. Acta 447 (2006) 89-100.
[8] A. Unal, A. V. Bradshaw, Metall. Trans. B 14 (1983) 743-752.
[9] M. Farren, S. P. Matthew, P. C. Hayes, Metall. Trans. B 21 (1990) 135-139.
[10] R. A. D. Rodriguez, A. N. Conejo, E. B. Bedolla, I&SM 30 (2003) 25-33.
[11] P. Zhao, P. M. Guo, D. W. Zhang, Iron and Steel 41 (2006) No. 8, 12-15.
[12] P. Zhao, P. M. Guo, in: CSM 2005 Annual Meeting Proceedings (Vol. 3), Metallurgical Industry Press, Beijing, 2005, pp. 677-681.
[13] P. Zhao, P. M. Guo, Iron and Steel 40 (2005) No. 6, 6-9.
[14] P. M. Guo, D. W. Zhang, P. Zhao, Spectroscopy and Spectral Analysis 27 (2007) 816-818.
[15] Y. X. Hua, Metallurgical Process Dynamics Introduction, Metallurgical Industry Press, Beijing, 2004.
[16] A. M. Squires, C. A. Johnson, J. Metals 1 (1957) 586-590.